ERJ open research
THE BEST IN OPEN ACCESS BASIC, TRANSLATIONAL & CLINICAL RESPIRATORY RESEARCH

Early View

Original research article

Nasal epithelial cell culture FRAP predicts cystic fibrosis therapeutic response

Timothy E Corcoran, Carol A Bertrand, Michael M. Myerburg, Daniel J. Weiner, Sheila A. Frizzell, Anna Li, Brittani Agostini, Robert S. Parker, R. Monica E. Shapiro, Ashok Muthukrishnan, Nicholas D. Hages, Brian P. Mulhern, Joseph M. Pilewski

Please cite this article as: Corcoran TE, Bertrand CA, Myerburg MM, *et al*. Nasal epithelial cell culture FRAP predicts cystic fibrosis therapeutic response. *ERJ Open Res* 2022; in press (https://doi.org/10.1183/23120541.00382-2022).

Nasal epithelial cell culture FRAP predicts cystic fibrosis therapeutic response

Timothy E Corcoran[1,2,3], Carol A Bertrand[4], Michael M. Myerburg[1], Daniel J. Weiner[5], Sheila A. Frizzell[1], Anna Li[6], Brittani Agostini[5], Robert S. Parker[2], R, Monica E. Shapiro[2], Ashok Muthukrishnan[7], Nicholas D. Hages[2], Brian P. Mulhern[1], Joseph M. Pilewski[1,4,8]

1-Division of Pulmonary, Allergy, and Critical Care Medicine, University of Pittsburgh, Pittsburgh, PA, USA
2-Department of Chemical and Petroleum Engineering, University of Pittsburgh, Pittsburgh, PA, USA
3-Department of Bioengineering, University of Pittsburgh, Pittsburgh, PA, USA
4-Department of Pediatrics, University of Pittsburgh, Pittsburgh, PA, USA
5- Division of Pediatric Pulmonology, University of Pittsburgh, Pittsburgh, PA, USA
6-School of Medicine, University of Pittsburgh, Pittsburgh, PA, USA
7- Department of Radiology, University of Pittsburgh, Pittsburgh, PA, USA
8-Department of Cell Biology, University of Pittsburgh, Pittsburgh, PA, USA

Corresponding Author:
Tim Corcoran, PhD
UPMC MUH NW628
3459 Fifth Ave.
Pittsburgh, PA 15213 USA

(412)624-8918
corcorante@upmc.edu

ABSTRACT:

Human nasal epithelial (HNE) cells can be sampled non-invasively and cultured to provide a model of the airway epithelium that reflects cystic fibrosis (CF) pathophysiology. We hypothesized that *in vitro* measures of HNE cell physiology would correlate directly with *in vivo* measures of lung physiology and therapeutic response, providing a framework for using HNEs for therapeutic development and precision medicine.

We sampled nasal cells from participants with CF (CF, n=26), healthy controls (HC, n=14), and the single mutation carrier parents of the CF group (CR, n=16). Participants underwent lung physiology and sweat chloride testing, and nuclear imaging-based measurement of mucociliary clearance (MCC) and small-molecule absorption (ABS). CF participants completed a second imaging day that included hypertonic saline (HS) inhalation to assess therapeutic response in terms of MCC. HNE measurements included Ussing chamber electrophysiology, small molecule and liquid absorption rates, and particle diffusion rates through the HNE airway surface liquid measured using fluorescence recovery after photobleaching (FRAP).

Long FRAP diffusion times were associated with increased MCC response to HS in CF. This implies a strong relationship between inherent factors affecting ASL mucin concentration and therapeutic response to a hydrating therapy. MCC decreased with age in the CR group which had a larger range of ages than the other two groups. Likely this indicates a general age-related effect that may be accentuated in this group. Measures of lung ABS correlated with sweat chloride in both the HC and CF groups indicating that CFTR function drives this measure of paracellular small-molecule probe absorption.

INTRODUCTION:

Human bronchial and nasal epithelial cell cultures have been used to study Cystic Fibrosis (CF) pathophysiology and to develop therapies for CF. Nasal epithelial cells (HNEs) can be sampled from the nose through minimally invasive procedures and demonstrate the characteristic pathophysiology of CF airways disease (1, 2). They also provide a means of comparing cell and organ level physiology and therapeutic response within the same subjects. HNE have received previous use for personalization of therapies (3).

We hypothesized that *in vitro* measures of HNE cell physiology would correlate directly with *in vivo* measures of therapeutic response in people with CF, providing a framework for using HNEs for therapeutic development and precision medicine. We collected and cultured HNE cells from participants with CF who then performed assessments of lung physiology at baseline and after the inhalation of 7% hypertonic saline (HS). HS is a common therapy applied in CF to hydrate secretions and improve mucus clearance. We also sought to determine whether there were direct correlations between measures of *in vivo* lung physiology and *in vitro* measures of HNE cell physiology. To obtain a wide range for physiological assessments we also performed HNE sampling and lung physiology measurements with healthy controls and some of the parents of the enrolled CF subjects who were carriers of a single disease-causing CFTR mutation.

HNE physiology measures included Ussing chamber assessments of Na^+ and Cl^- currents, and transepithelial resistance (TER), particle diffusion rates through the HNE airway surface liquid (ASL) made using fluorescence recovery after photobleaching (FRAP)(4, 5), optical measures of ASL absorption rate (6), and measurements of small molecule absorption made using radiolabeled probes (cell ABS) (7).

Lung and systemic physiology measurements included sweat chloride, spirometry, multiple-breath washout testing, and nuclear imaging-based measurements of mucociliary clearance (MCC) (8), and small molecule absorption (ABS)(9, 10). MCC measures the clearance rate of an inhaled radiolabeled non-absorbable probe (Technetium 99m sulfur colloid) from the lungs as a surrogate for mucus clearance. Therapeutic response was assessed as the increase in MCC after the inhalation of HS vs. baseline. ABS measures the absorption rate of a small-molecule radiolabeled probe (Indium111 DTPA) from the lung. This measure was initially developed as an *in vivo* surrogate for detecting changes in ASL absorption. It provides a measure of paracellular transport likely affected by both paracellular liquid absorption and permeability. Previous studies have demonstrated that ABS is increased in the CF lung and increases proportionally with sweat chloride (11).

METHODS:

General Study Procedures:

We enrolled participants with CF from our regional center in Pittsburgh who were 12 years old or older with FEV_1 % pred $\geq$30% (CF), their single CFTR mutation-carrier biological parents (CR), and healthy controls who were 18 years old or older with FEV_1 % pred $\geq$70% (HC). Subjects were excluded if they were pregnant or nursing, smokers, or using e-cigarettes. Subjects in the HC group provided blood samples and were excluded if they carried one of 144 known disease-causing CFTR mutations. Recruitment occurred from early 2017 through late 2019.

The HC and CR groups performed a single study visit that included nasal cell sampling, pulmonary function testing and multiple-breath washout (MBW), sweat chloride measurement, and a two-probe nuclear scan to assess MCC/ABS. Nebulized isotonic saline (IS) was delivered for 10 minutes after the first 10 minutes of the MCC/ABS scan as a stimulus for liquid absorption in the airways.

Participants in the CF group performed one study day where they inhaled nebulized IS and a second study day where they inhaled nebulized HS during the MCC/ABS measurement. The order of the HS and IS days was randomized and the studies were separated by 7-14 days. The study was approved by the University of Pittsburgh Institutional Review Board and registered at clinicaltrials.gov as NCT02947126. Funding was through NIH 1 UO1 HL131046-01.

Nasal cell sampling, culturing, and testing:

During nasal cell sampling, a standard otoscope was used to visualize the inferior turbinate and a cytology brush was used to collect cells from along the lower aspect of the turbinate in both nostrils. Culturing methods are described in the supplement. Ussing chamber studies were performed on the HNE cultures including measurements of Chloride (Cl^-) and Sodium (Na^+) currents and transepithelial resistance (TER). (Na+ current was determined using amiloride to block ENaC. Cl- current was measured after forskolin activation of CFTR.) We also measured the absorption rate of the gamma emitting small molecule Technetium 99m Diethylenetriamine pentaacetate (Tc-DTPA) from the apical surface of the HNEs (Cell ABS). This *in vitro* measurement parallels the *in vivo* measurement of Indium 111-DTPA absorption in the MCC/ABS scans. HNE cultures were not treated with any CFTR modulators and thus the *in vitro* measurements do not reflect modulator use. More detailed methods are included in the supplement.

FRAP was used to measure the diffusion rate of 70 kDa FITC-labeled dextran through the ASL layer. Procedures were performed as previously described (4, 12). Detailed FRAP methods are included in the supplement. The physiological relevance of this measurement has been previously described (13). FRAP is presented as a ratio of the ASL diffusion time relative to that of saline.

Measurements of lung physiology and sweat chloride:

Participants performed nuclear scans to measure mucociliary clearance (MCC) and small molecule probe absorption (ABS). Subjects inhaled a combination of Technetium 99m sulfur colloid and Indium 111 DTPA in a nebulized liquid aerosol and sequential gamma camera images were collected for 80 minutes. All participants inhaled nebulized isotonic saline for 10 minutes starting 10 minutes into the imaging period while imaging continued. On a separate study day (order randomized) the CF group inhaled 7% hypertonic saline (Pulmosal) during this period instead of isotonic saline.

Previous studies have demonstrated that differences in the initial distribution of the deposited radioisotope aerosol in the lung can have a confounding effect on measurements of MCC (10). To facilitate comparisons of MCC measurements on different days with potentially different aerosol distributions, we calculated a measure of MCC that was adjusted based on the initial deposition of the radioisotope aerosol ($MCC_{adjusted}$). More details on the imaging methods and MCC adjustment are included in the supplement. Therapeutic response was defined as the increase $MCC_{adjusted}$ on the HS day vs. the baseline IS day.

Details of sweat chloride measurement are included in the supplement. Multiple-breath washout methods are included in the supplement and data on Lung Clearance Index (LCI) is presented.

Statistics:

In vitro and *in vivo* continuous variables were compared between the CF, CR, and HC groups using Kruskal-Wallis (non-parametric) testing including all 3 groups followed by individual group comparisons by Dunn's test with Holm adjustment (non-parametric, multiple comparisons). A similar analysis was done to compare the effects of the use of CFTR modulators within the CF group. Sex and culture success rates were compared with Chi-Squared. HS vs IS comparisons of

imaging outcomes in CF group were performed using the Wilcoxon matched-pairs signed-ranks test (non-parametric, paired). Multivariable linear regression was used to determine the effects of aerosol distribution and testing group on MCC. Univariant regression was used to assess relationships between *in vitro* and *in vivo* variables and therapeutic response. Univariant regression was used to assess relationships between *in vitro* and *in vivo* variables baseline MCC. Multivariable regression was used to model FEV1%p in the CF group. For all regressions, a robust variance estimator was used, and the normality of the residuals was verified with Shapiro-Wilk W test. Analysis was performed using Stata/IC 14.0 (RRID:SCR_012763, StataCorp LP, College Station, TX, USA).

RESULTS:

Participant demographics, pulmonary function, multiple-breath washout, and sweat chloride measurements are included in **Table 1.** As expected, CF was associated with increased sweat chloride, decreased pulmonary function, and increased LCI. Sweat chloride in the single-mutation carrier group (CR) was similar to previous reports (14). No CR subjects had sweat chloride measurements > 60 mMol/L. The CR group was significantly older than the other groups. 11 participants in the CF group had chronic *Pseudomonas aeruginosa* (PA) infection, defined here as 2 or more positive throat or sputum cultures in the previous year.

Table 2 compares cell physiology and electrophysiology in the CF, CR, and HC nasal cell cultures. Culturing success in the CR group was limited with just over 50% of cell samples producing successful cultures. CF subjects demonstrated the expected low Cl^- currents along with increased liquid absorption rates, Cell ABS, and FRAP vs. HC. Na^+ currents were significantly lower in the CR group compared to the HCs. There were no significant differences in Cl- currents, liquid absorption rate, cell ABS, or FRAP when comparing CR to HC. TER was similar in all three groups.

Table 3 compares *in vivo* measures of MCC and ABS in the CF, HC, and CR groups made after IS saline inhalation. MCC measurements in Table 3 are not adjusted for aerosol distribution. MCC was similar in all three groups. ABS was higher in CF vs HC matching previous results (15) (16). The CF subjects also performed a second study day where they inhaled 7% hypertonic saline during the MCC/ABS measurement. As anticipated, HS inhalation increased MCC. Whole lung ABS did not decrease with HS inhalation as it had in previous studies (16), but peripheral lung ABS did decrease with HS use.

A comparison of the *in vitro* and *in vivo* variables based on CFTR modulator use is included in the supplement (**Table S1**). Four subjects were using ivacaftor, 3 lumacaftor/ivacaftor, 4 tezacaftor/ivacaftor, 14 did not use modulators, and 1 had unknown status. The study predated the approval of elexacaftor. We compared subjects in 3 groups: (1) ivacaftor (n=4), (2) lumacaftor or tezacaftor (n=7), and (3) no CFTR modulator (n=14). Sweat chloride was significantly lower with ivacaftor group compared to those not using modulators.

In previous studies radioisotope aerosol distribution has been shown to affect the MCC measurement with high central lung deposition resulting in higher MCC measurements. In **Table S2** we show the results of multivariable regression models demonstrating this effect in whole and peripheral lung MCC measurements. Central lung deposition percentage was used as a measure of aerosol distribution. Both whole lung and peripheral lung MCC increased with central deposition percentage ($p<0.001$, $p=0.02$ respectively). MCC did not significantly vary by group (CR, CF vs. HC).

Therapeutic response was defined here as the increase in MCC after inhalation of HS vs. a baseline measurement made after IS inhalation. To facilitate comparisons of therapeutic response we calculated an "adjusted" whole lung MCC value that accounts for the effect of aerosol distribution patterns thus allowing for easier comparisons between different days with potentially different initial aerosol distributions. Measures of central aerosol deposition percentage are used to adjust

MCC. Details of this calculation are included in the supplement and values of $MCC_{adjusted}$ are shown in **Table S3**. Median therapeutic response ($MCC_{adjusted}$ HS day – $MCC_{adjusted}$ IS day) was 17%, IQR: 8-28%, range: -24 to +50%.

We considered whether any *in vivo* measurements associated with therapeutic response. Not surprisingly, subjects with lower baseline MCC values had more therapeutic response to HS inhalation. There was no relationship between response and age, FEV1, FVC, FEF25-75, LCI, sweat chloride, or ABS. We also considered whether any *in vitro* measurements were associated with therapeutic response. Cl- current, Na+ current, i-ratio, TER, cell ABS, and HNE normalized liquid absorption rate were not. Therapeutic response increased with FRAP as shown in **Figure 1.** FRAP is a measure of particle diffusion through the ASL. Longer FRAP diffusion times have been associated with higher ASL solids concentrations (13). Our result implies a strong relationship between inherent factors affecting ASL mucin concentration, as assessed *in vitro,* and *in vivo* therapeutic response to a hydrating therapy. Normalized liquid absorption rate was weakly associated with FRAP in the CF HNE (R^2=0.33, p=0.07) as shown in **Figure 2.** Factors in addition to dehydration may also contribute to increasing FRAP. Model coefficients and associated values for R^2 and p are included in **Table 4**.

Comparing *in vitro* and *in vivo* physiology, we considered whether any *in vivo* measures were associated with baseline $MCC_{adjusted}$ in any of the three groups. There was no relationship with FEV1, FVC, FEF25-75, LCI, or sweat chloride in any of the groups. There was no difference in $MCC_{adjusted}$ based on sex in any of the groups. Contrary to previous outcomes (8, 10, 17), there was no difference in $MCC_{adjusted}$ based on chronic *Pseudomonas aeruginosa* (PA) in the CF group. $MCC_{adjusted}$ decreased significantly with age in the CR group which had a wider range of ages than the CR or CF groups (range: 35-73 years) as shown in **Figure 3.** Decreases in MCC with age have been reported previously in healthy controls (18). There was no association between $MCC_{adjusted}$

and Cl- current, Na+ current, i-ratio, FRAP, TER, or HNE normalized liquid absorption rate in any of the groups.

We considered multivariable models of FEV1%p in the CF group in **Table 5**. We included baseline factors of age, chronic PA infection, gender, and sweat chloride which reflects both the baseline severity of CFTR dysfunction and correction of this defect with CFTR modulators. The baseline model accounted for 66% of the variation in FEV1% in a highly significant model (row 1, R^2=0.66). The only *in vitro* variable that provided substantial improvement of this correlation was FRAP. Since not all subjects had FRAP measurements, this effectively decreased the size of the data set to n=10 but did increase R^2 to 0.91 (row 2). The baseline model run with the same 10 subjects yielded an R^2=0.76 (row 3).

There were no relationships between lung ABS and measured *in vitro* variables: cell ABS, Cl^- current, normalized liquid absorption rate, or TER, in any of the groups. Cell ABS increased with airway surface liquid absorption rate *in vitro* (R^2=0.14, p=0.002, n=37) in agreement with previous reports (7). There was a correlation between lung ABS and sweat chloride in both the CF (R^2=0.19, p=0.002) and HC groups (R^2=0.60, p=0.01). Our group had previously reported similar correlations in CF (9). There was no correlation in the CR group. Here much of the relationship in the CF group was driven by subjects with low ABS and sweat chloride values associated with the use of CFTR modulators. ABS is a measure of the paracellular absorption of a small molecule radiolabeled probe in the lung. This result indicates that this process is highly influenced by CFTR function in both healthy and CF lungs, likely moderated by paracellular liquid absorption.

DISCUSSION:

Here we hypothesized that *in vitro* measures of HNE cell physiology would correlate with *in vivo* measures of therapeutic response and lung physiology, providing a framework for using HNEs for therapeutic development and personalization.

In vivo therapeutic response to HS inhalation increased with FRAP diffusion time in the CF group. FRAP was measured using 70 kDa fluorescent dextran particles which are significantly smaller than the mesh size of the mucin network in the ASL. Previous studies have associated the diffusion time of small particle probes with the viscosity of the solvent component of the mucus gel (13). Here FRAP is likely driven by ASL solids concentrations which could be affected by mucus secretion or hydration. FRAP was only weakly correlated with ASL absorption rate suggesting that differences in mucus secretion may also be involved. Differences in mucin binding could also play a role. Previous studies have demonstrated a pH effect on FRAP associated with changes in electrostatic bonds between mucins. These studies also demonstrated Ca+ dependent effects on FRAP (19). Our results indicate that the inherent airway mucus composition and hydration characteristics of a patient can be characterized through measurements of HNE FRAP and used to predict the utility of hydrating therapies like HS. This relationship exists independent of CFTR modulator use which is not reflected in HNE cultures.

We sought to determine whether any *in vitro* measures correlated directly with *in vivo* measures or organ level physiology in the lungs in any of the 3 participant groups. No *in vitro* measures consistently with baseline MCC. In considering the relationship between other patient variables and MCC we noted clear relationship between age and MCC in the CR group which included the CF carrier parents of the CF group. It is unknown if this effect is unique to this group, or a more general effect of aging illustrated here based on the wide range of ages within CR. Previous studies have noted decreases in MCC with age in humans and mice (18, 20-22). Studies have indicated that

single CFTR mutation carriers may be at higher risk of conditions such as pancreatitis, bronchiectasis, diabetes, constipation, and cholelithiasis (23), as well as bronchitis and lung cancer (24). The relationship between age and decreasing MCC merits further examination since this important host defense prevents obstruction and limits exposure to inhaled pathogens and toxins (including cigarette smoke). A decrease in MCC with age would indicate increased vulnerability to these effects.

We considered whether any *in vitro* measures correlated with measures of FEV1%p in the CF group using multivariable models including factors known to affect pulmonary function in this group: age, chronic PA infection, and gender (25). We also included sweat chloride as a measure of both the severity of the baseline CFTR defect and to capture the function correction associated with CFTR modulators. This baseline model accounted for 66% of the variation in FEV1%p. Addition of FRAP to this model significantly improved correlation though only a very limited dataset was available for use (n=10).

Our imaging measurements included a measurement of small molecule absorption (ABS). This technique was developed to detect changes in ASL absorption in the airways and has been previously described. These studies confirmed previously described increases in ABS in CF and correlation between ABS and sweat chloride in CF (10, 11, 15). We also noted correlation between ABS and sweat chloride in the HC group. These results indicate an influence of CFTR driven liquid absorption on this imaging biomarker in both CF patients and healthy controls.

Limitations of our study include the small numbers of assessments in some groups. Culturing cells from the CR group was particularly challenging and limited our ability to assess this group. Our study also did not include a validation dataset which limits the utility of the models presented.

Overall, our results demonstrate the utility of HNE cultures for assessing therapeutic response for hydrating therapies. *In vitro* measurements of FRAP were particularly useful for predicting response and for characterizing important properties of ASL mucus that were ultimately reflected in lung physiology. Further studies are required to determine the applicability of FRAP for assessing other therapies and to better understand the pathophysiological mechanisms reflected in the measurement.

	CF (n=26)	CR (n=16)	HC (n=14)	p	p (CFvHC)	p (CFvCR)	p (CRvHC)
Age (years)	26.5 (19-39)	48.0 (44-63.5)	22.5 (20-23)	0.0001	0.09	<0.0001	<0.0001
Female/male	14/12	10/6	6/8	0.56	0.51	0.29	0.43
FEV_1 % pred	70 (50-93)	97 (93-109)	102 (95.5-113) n=12	0.0003	0.0008	0.0014	0.30
FVC % pred	94.5 (76-104)	104.0 (96-109)	107.5 (100-116) n=12	0.02	0.01	0.05	0.23
FEF_{2575} % pred	40.5 (22-66)	100.5 (74-119.5)	83.0 (68-99.5) n=12	0.0001	0.004	0.0002	0.29
LCI	9.0 (7.6-13) n=23	7.8 (7.1-8.3)	7.2 (6.7-7.5) n=11	0.0007	0.0005	0.01	0.10
Sweat Chloride (mMol/L)	101 (91-110)	36 (21-53) n=14	22 (10-29) n=12	0.0001	<0.0001	0.0002	0.11

Table 1: Demographics of study participants along with pulmonary function, lung clearance index (LCI), and sweat chloride data. Data is Median (interquartile range). P values comparing all groups by Kruskal-Wallis (non-parametric) except sex which is chi-squared. Group comparisons by Dunn's test with Holm adjustment (non-parametric, multiple comparisons).

CF=cystic fibrosis, CR=single CFTR mutation carrier, HC=healthy controls, FEV1% pred = one-second forced expiratory volume % of predicted value, FVC% pred = forced vital capacity % of predicted, FEF2575 % pred = forced expiratory flow at 25-75% of FVC, % of predicted. LCI=lung clearance index from multi-breath washout testing.

	CF (n=26)	CR (n=16)	HC (n=14)	p	p (CFvHC)	p (CFvCR)	P (CRvHC)
Culture success/failed	23/3	9/7	14/0	0.004	0.18	0.004	0.001
Cl^- current ($\mu A/cm^2$)	0.21 (-0.2-0.5) n=16	4.0 (1.5-5.2) n=7	5.4 (4.9-10.2) n=13	0.0001	<0.0001	0.003	0.13
Na^+ current ($\mu A/cm^2$)	22.1 (7.8-41.3) n=16	9.3 (2.5-18.4) n=7	37.2 (26.0-46.9) n=13	0.012	0.10	0.04	0.004
i ratio (Na^+ current/ Cl^- current)	29.4 (-3.9-112.3) n=16	1.2 (0.7-3.9) n=7	6.0 (4.2-8.0) n=13	0.03	0.06	0.02	0.18
TER (Ohm cm^2)	651 (453-807) n=16	717 (205-1066) n=7	556 (499-673) n=13	0.63	0.50	0.37	0.66
Cell ABS (% cleared/ 24 hours)	49.7 (38.2-54.1) n=23	42.4 (35.6-54.3) n=9	36.8 (27.1-45.2) n=14	0.03	0.01	0.19	0.22
Normalized Liquid Absorption Rate (%/24hrs)	68.4 (61.2-80.2) n=17	53.7 (39.5-72.5) n=7	59.4 (37.2-66.5) n=13	0.03	0.02	0.11	0.31
HNE ASL FRAP diffusion Time (τ/τ_{saline})	3.5 (2.8-4.0) n=10	2.7 (1.2-3.0) n=5	2.1 (1.3-3.1) n=13	0.03	0.02	0.08	0.40

Table 2: *In vitro* measures of nasal epithelial cell physiology. Cl^- and Na^+ currents and TER measured using Ussing chamber. Cell ABS is the absorption rate of Technetium 99m -DTPA from the apical surface of the cultures after addition in a 10 µL volume. Liquid absorption is measured via an optical technique (5) based on changes in ASL volume after 10 µL volume addition. Not all sampled cultures were viable and available for all measurements. Data presented graphically in supplemental Figure S3.

Data is Median (interquartile range). P values comparing all groups by Kruskal-Wallis (non-parametric) except for culture success/failure which is Chi-squared. Group comparisons by Dunn's test with Holm adjustment (non-parametric, multiple comparisons). The number of individual cell donors is listed as n. A minimum of 3 cultures is included in each measurement.

ABS=Technetium 99m DTPA absorption rate, ASL=airway surface liquid, CF=cystic fibrosis, CR=single disease-causing CFTR mutation carrier, HC=healthy controls, HNE=human nasal epithelial cell cultures, TER=transepithelial resistance. FRAP = fluorescence recovery after photobleaching.

	CF (n=26) IS	CR (n=16)	HC (n=12)	CF (n=26) HS	p	p(CFvHC)	p(CFvCR)	p(CRvHC)	p CF (HSvIS)
MCC (WL)	38 (26-49)	36 (30-43)	36 (26-47)	55 (35-70)	0.97	0.49	1.00	0.83	0.0001
MCC (PL)	36 (16-43)	35 (31-39)	35 (28-43)	54 (35-62)	0.81	0.84	0.63	0.44	<0.0001
ABS (WL)	21 (8-26)	13 (7-24)	6 (0-13)	18 (6-25)	0.03	0.01	0.14	0.14	0.21
ABS (PL)	20 (11-32)	17 (5-22)	7 (0-18)	14 (8-25)	0.05	0.03	0.15	0.16	0.03
Cen %	51 (47-57)	52 (48-57)	49 (46-51)	52 (48-56)	0.22	0.14	0.43	0.16	0.83

Table 3: Imaging-based measurements across the groups. All groups inhaled isotonic saline (IS) during the MCC/ABS scan. CF subjects performed an additional study day where they inhaled 7% hypertonic saline (HS) during the scan. Data presented graphically in supplemental Figures S4 and S5 (CF HS vs IS).

Data is Median (interquartile range). P values comparing all groups by Kruskal-Wallis (non-parametric). Group comparisons by Dunn's test with Holm adjustment (non-parametric, multiple comparisons). HS vs IS comparison for CF group by Wilcoxon matched-pairs signed-ranks test (non-parametric, paired).

ABS=Technetium 99m DTPA absorption rate, Cen% = percentage of radioactive counts deposited in the central lung zone (see supplement), CF=cystic fibrosis, CR=single disease-causing CFTR mutation carrier, HC=healthy controls, MCC=mucociliary clearance rate, PL=peripheral lung, WL=whole lung.

	β0	β1	R^2	p
Baseline $MCC_{adjusted}$	31.62	-0.44	0.20	0.01
HNE ASL FRAP diffusion time	-23.52	11.23	0.55	0.04

Table 4: Variables that correlated with therapeutic response to hypertonic saline (HS) in the CF group. Therapeutic response is the improvement in $MCC_{adjusted}$ after inhaling HS compared to a baseline measurement made after IS inhalation.

Therapeutic response = β1 (listed variable) + β0.

ASL=airway surface liquid, CF=cystic fibrosis, HNE=human nasal epithelial cell cultures, FRAP = fluorescence recovery after photobleaching, $MCC_{adjusted}$=mucociliary clearance adjusted based on aerosol distribution.

Model Number	Group	Model of	Age (years)		Chronic PA		Sex (female)		Sweat Chloride (mMol/L)		HNE ASL FRAP		Model		
			β1	p	β2	p	β3	p	β4	p	β5	p	R^2	p	β 0
1	CF	FEV_1% pred (n=25)	-1.1	0.001	-22.7	0.007	-10.9	0.12	-0.26	0.05	-	-	**0.66**	**<0.0001**	145
2	CF	FEV_1%p (n=10)*	-0.85	0.11	-30.0	0.09	-27.8	0.03	-0.21	0.45	-13.8	0.02	**0.91**	**0.01**	187
3	CF	FEV1%p (n=10)*	-1.1	0.09	-7.95	0.70	-24.8	0.07	-0.25	0.57			**0.76**	**0.03**	142

Table 5: Multivariable regression models of FEV_1% pred in the CF group.

FEV1%p = β1 (age) + β2(PA) + β3(Sex) + β4(sweat chloride) + β5(FRAP) + β0.

*-Only a portion of the CF group had FRAP measurements available (n=10). MCC=mucociliary clearance, FEV_1% pred =one-second force expiratory volume percent of predicted. PA=*Pseudomonas aeruginosa*. Chronic PA is defined as 2 or more positive throat or sputum cultures in the previous year. HNE=human nasal epithelial cell cultures. ASL=airway surface liquid. FRAP = fluorescence recovery after photobleaching.

References

1. de Courcey F, Zholos AV, Atherton-Watson H, Williams MT, Canning P, Danahay HL, Elborn JS, Ennis M. Development of primary human nasal epithelial cell cultures for the study of cystic fibrosis pathophysiology. *American journal of physiology* 2012; 303: C1173-1179.

2. van Meegen MA, Terheggen-Lagro SW, Koymans KJ, van der Ent CK, Beekman JM. Apical CFTR expression in human nasal epithelium correlates with lung disease in cystic fibrosis. *PloS one* 2013; 8: e57617.

3. McCarthy C, Brewington JJ, Harkness B, Clancy JP, Trapnell BC. Personalised CFTR pharmacotherapeutic response testing and therapy of cystic fibrosis. *Eur Respir J* 2018; 51.

4. Lennox AT, Coburn SL, Leech JA, Heidrich EM, Kleyman TR, Wenzel SE, Pilewski JM, Corcoran TE, Myerburg MM. ATP12A promotes mucus dysfunction during Type 2 airway inflammation. *Scientific reports* 2018; 8: 2109.

5. Hill DB, Long RF, Kissner WJ, Atieh E, Garbarine IC, Markovetz MR, Fontana NC, Christy M, Habibpour M, Tarran R, Forest MG, Boucher RC, Button B. Pathological mucus and impaired mucus clearance in cystic fibrosis patients result from increased concentration, not altered pH. *Eur Respir J* 2018; 52.

6. Harvey PR, Tarran R, Garoff S, Myerburg MM. Measurement of the airway surface liquid volume with simple light refraction microscopy. *Am J Respir Cell Mol Biol* 2011; 45: 592-599.

7. Corcoran TE, Thomas KM, Brown S, Myerburg MM, Locke LW, Pilewski JM. Liquid hyper-absorption as a cause of increased DTPA clearance in the cystic fibrosis airway. *EJNMMI Res* 2013; 3: 14.

8. Donaldson SH, Laube BL, Corcoran TE, Bhambhvani P, Zeman K, Ceppe A, Zeitlin PL, Mogayzel PJ, Jr., Boyle M, Locke LW, Myerburg MM, Pilewski JM, Flanagan B, Rowe SM, Bennett WD. Effect of ivacaftor on mucociliary clearance and clinical outcomes in cystic fibrosis patients with G551D-CFTR. *JCI Insight* 2018; 3.

9. Corcoran TE, Huber AS, Myerburg MM, Weiner DJ, Locke LW, Lacy RT, Weber L, Czachowski MR, Johnston DJ, Muthukrishnan A, Lennox AT, Pilewski JM. Multiprobe Nuclear Imaging of the Cystic Fibrosis Lung as a Biomarker of Therapeutic Effect. *Journal of aerosol medicine and pulmonary drug delivery* 2019.

10. Locke LW, Myerburg MM, Weiner DJ, Markovetz MR, Parker RS, Muthukrishnan A, Weber L, Czachowski MR, Lacy RT, Pilewski JM, Corcoran TE. Pseudomonas infection and mucociliary and absorptive clearance in the cystic fibrosis lung. *Eur Respir J* 2016; 47: 1392-1401.

11. Corcoran TE, Huber AS, Myerburg MM, Weiner DJ, Locke LW, Lacy RT, Weber L, Czachowski MR, Johnston DJ, Muthukrishnan A, Lennox AT, Pilewski JM. Multiprobe Nuclear Imaging of the Cystic Fibrosis Lung as a Biomarker of Therapeutic Effect. *J Aerosol Med Pulm Drug Deliv* 2019; 32: 242-249.

12. Derichs N, Jin BJ, Song Y, Finkbeiner WE, Verkman AS. Hyperviscous airway periciliary and mucous liquid layers in cystic fibrosis measured by confocal fluorescence photobleaching. *FASEB J* 2011; 25: 2325-2332.

13. Hill DB, Long RF, Kissner WJ, Atieh E, Garbarine IC, Markovetz MR, Fontana NC, Christy M, Habibpour M, Tarran R, Gregory Forest M, Boucher RC, Button B. Pathological Mucus and Impaired Mucus Clearance in Cystic Fibrosis Patients Results from Increased Concentration, not altered pH. *Eur Respir J* 2018.

14. Colin AA, Sawyer SM, Mickle JE, Oates RD, Milunsky A, Amos JA. Pulmonary function and clinical observations in men with congenital bilateral absence of the vas deferens. *Chest* 1996; 110: 440-445.

15. Corcoran TE, Thomas KM, Myerburg MM, Muthukrishnan A, Weber L, Frizzell R, Pilewski JM. Absorptive clearance of DTPA as an aerosol-based biomarker in the cystic fibrosis airway. *Eur Respir J* 2010; 35: 781-786.

16. Locke LW, Myerburg MM, Markovetz MR, Parker RS, Weber L, Czachowski MR, Harding TJ, Brown SL, Nero JA, Pilewski JM, Corcoran TE. Quantitative imaging of airway liquid absorption in cystic fibrosis. *Eur Respir J* 2014; 44: 675-684.

17. Laube BL, Sharpless G, Benson J, Carson KA, Mogayzel PJ, Jr. Mucus Removal Is Impaired in Children with Cystic Fibrosis Who Have Been Infected by Pseudomonas aeruginosa. *The Journal of pediatrics* 2014; 164: 839-845.

18. Svartengren M, Falk R, Philipson K. Long-term clearance from small airways decreases with age. *Eur Respir J* 2005; 26: 609-615.

19. Tang XX, Ostedgaard LS, Hoegger MJ, Moninger TO, Karp PH, McMenimen JD, Choudhury B, Varki A, Stoltz DA, Welsh MJ. Acidic pH increases airway surface liquid viscosity in cystic fibrosis. *J Clin Invest* 2016; 126: 879-891.

20. Grubb BR, Livraghi-Butrico A, Rogers TD, Yin W, Button B, Ostrowski LE. Reduced mucociliary clearance in old mice is associated with a decrease in Muc5b mucin. *Am J Physiol Lung Cell Mol Physiol* 2016; 310: L860-867.

21. Proenca de Oliveira-Maul J, Barbosa de Carvalho H, Goto DM, Maia RM, Flo C, Barnabe V, Franco DR, Benabou S, Perracini MR, Jacob-Filho W, Saldiva PHN, Lorenzi-Filho G, Rubin BK, Nakagawa NK. Aging, diabetes, and hypertension are associated with decreased nasal mucociliary clearance. *Chest* 2013; 143: 1091-1097.

22. Bailey KL, Bonasera SJ, Wilderdyke M, Hanisch BW, Pavlik JA, DeVasure J, Robinson JE, Sisson JH, Wyatt TA. Aging causes a slowing in ciliary beat frequency, mediated by PKCepsilon. *Am J Physiol Lung Cell Mol Physiol* 2014; 306: L584-589.

23. Miller AC, Comellas AP, Hornick DB, Stoltz DA, Cavanaugh JE, Gerke AK, Welsh MJ, Zabner J, Polgreen PM. Cystic fibrosis carriers are at increased risk for a wide range of cystic fibrosis-related conditions. *Proc Natl Acad Sci U S A* 2020; 117: 1621-1627.

24. Colak Y, Nordestgaard BG, Afzal S. Morbidity and mortality in carriers of the cystic fibrosis mutation CFTR Phe508del in the general population. *Eur Respir J* 2020; 56.

25. Gecili E, Brokamp C, Palipana A, Huang R, Andrinopoulou ER, Pestian T, Rasnick E, Keogh RH, Ni Y, Clancy JP, Ryan P, Szczesniak RD. Seasonal variation of lung function in cystic fibrosis: longitudinal modeling to compare a Midwest US cohort to international populations. *Sci Total Environ* 2021; 776.

The authors have nothing to disclose.

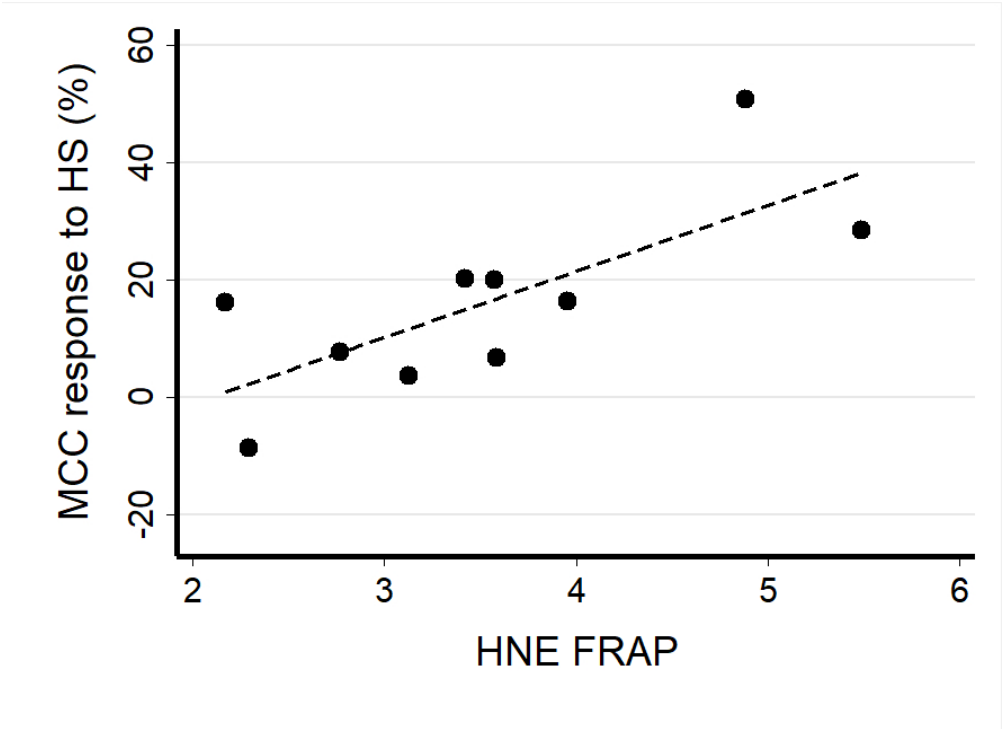

Figure 1: In vivo mucociliary clearance response to hypertonic saline inhalation correlates with in vitro measures of FRAP diffusion time measured in HNE cell cultures from the CF participants (R2=0.55, p=0.04). Only a portion of the CF group had FRAP measurements available (n=10).

MCC=mucociliary clearance. HNE=human nasal epithelial cell cultures. FRAP = fluorescence recovery after photobleaching.

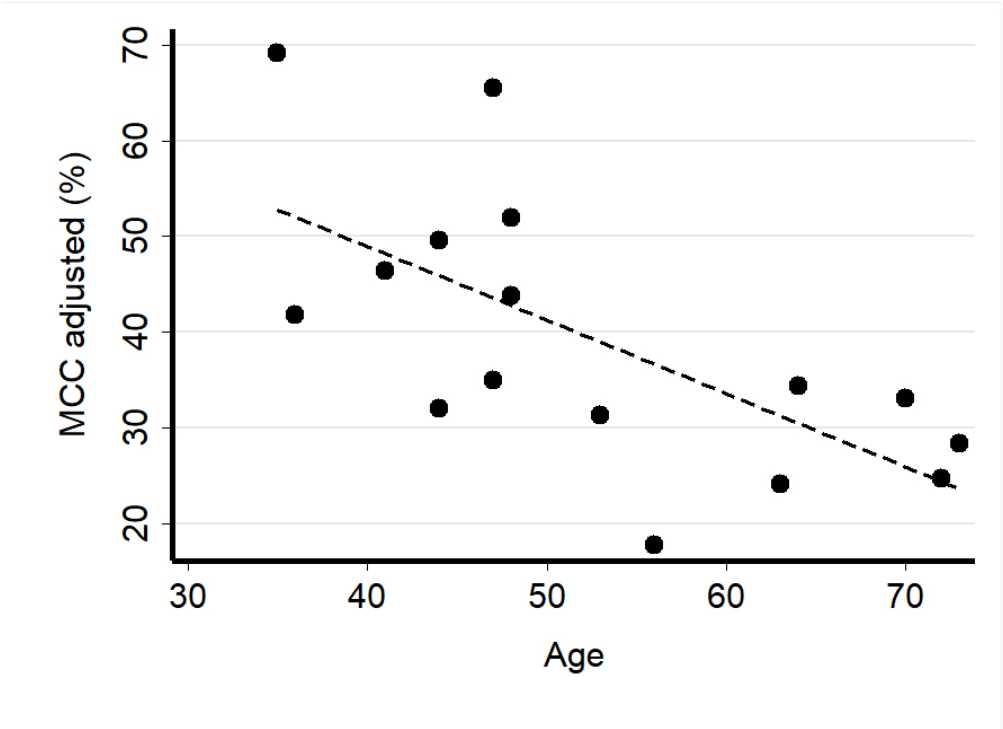

Figure 3: Mucociliary clearance (MCC) rate decreases with age in single CFTR mutation carriers (CR) (R2=0.44, p=0.002, n=16).

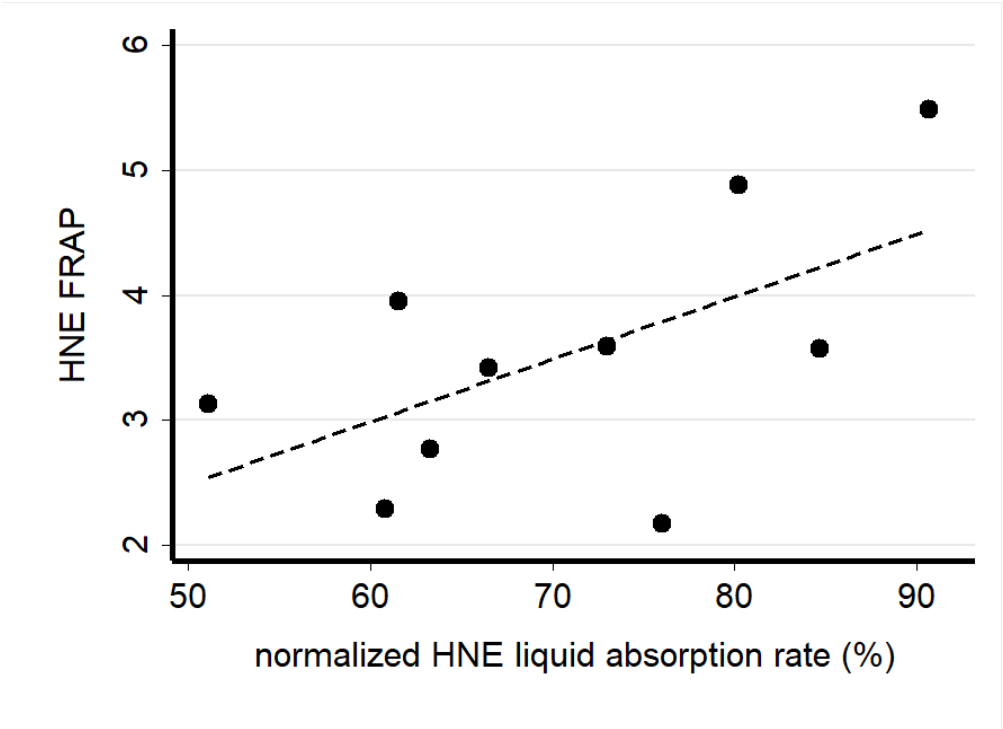

Figure 2: Relationship between FRAP diffusion time and airway surface liquid absorption rate in CF HNE cultures (R2=0.34, p=0.07). Only a portion of the CF group had FRAP measurements available (n=10). HNE=human nasal epithelial cell cultures. FRAP = fluorescence recovery after photobleaching.

Methods and Data Supplement:

Human Nasal Epithelial (HNE) cell sampling and culturing:

Subjects were asked to blow their nose before the sampling. A standard otoscope was used to visualize the inferior turbinate and a cytology brush was used to collect cells from along the lower aspect of the turbinate in both nostrils. The cytology brushes were placed in a 15 mL centrifuge tube containing sterile, ice-cold PBS, maintained on ice, and processed within 1 hour of sampling. In a sterile tissue culture hood, cells were dislodged from brushes by gently rubbing the brushes together, pelleted, and resuspended in Accutase for 10 min at 4 °C with rocking. Accutase was aspirated following centrifugation, and cells resuspended in "Georgetown" media in preparation for expansion.

Human nasal epithelial cells (HNEs) were expanded through co-culture with irradiated, 3T3 J2 feeder cells (irrJ2's), prepared ahead of nasal sampling. One day before sampling, two 100 ml petri dishes per subject were coated with 1x10^6 irrJ2's suspended in 10 ml/plate complete growth media and incubated in a 37 °C tissue culture incubator. After the fresh HNE were prepared, the complete growth media was aspirated from the petri dishes and replaced with 10 ml of the HNE preparation. Plates were returned to the 37 °C incubator and fed daily with Georgetown media. After the HNE cells reached 98% confluency, a second expansion phase was performed. HNE were dissociated from the original 2 plates with 0.05% trypsin, distributed to four 100 ml petri dishes precoated with irrJ2's, and maintained at 37 °C with daily feeding until 98% confluent.

Upon reaching 98% confluency, HNE were trypsinized (0.05%) from the plates and resuspended in BEGM, then seeded onto collagen-coated 0.33-cm^2 Costar Transwell filters at a density of 2 x $10^5/cm^2$; apical media was removed 24 hours after seeding and the filters grown at an air-liquid interface thereafter. Filters were fed 3x weekly with BEGM + Ultroser G differentiation media and used in assays between 0.5 and 2 months of seeding.

Media Composition:

Georgetown Media: Complete Growth Media(1x): 500 mL DMEM (H) (Gibco #11965-092) + 50 mL fetal bovine serum (Gibco #16140-071) + 5.5 mL 100x glutamine (Gibco #25030-081) + 5.5 mL pen/strep (Gibco #15140-122). Sterile. Store at 4°C.; F-12 Nutrient Mix (1x): Gibco #11765-054. Sterile. Store at 4°C. Hydrocortisone/EGF Mix (1000x): Dissolve hydrocortisone (Sigma H0888) in 100% ethanol at 0.5mg/ml. Mix 1 mL of this with 19 mL DMEM containing 2.5 ug EGF (Invitrogen PHG0311 or PHG0311L). Store sterile 1.1 mL aliquots at -20°C (hydrocortisone= 25 ug/mL; EGF=0.125 ug/mL). Insulin (5mg/mL): Dissolve 100 mg insulin (Sigma I5500 or I2643) in 20 mL distilled water containing 200 uL glacial acetic acid. Filter sterilize and store 1.1 mL aliquots at -20°C. Fungizone/Amphotericin B (250 ug/mL): Fisher #BP264550. Store sterile 1.1 mL aliquots at -20°C. Gentamicin (10 mg/ml): Gibco #15710-064. Sterile. Store at room temperature. Cholera toxin (11.7 uM): Dissolve 1 mg vial of cholera toxin (Sigma C8052) in 1 mL distilled water and filter sterilize. Stable at 4°C for one year. Y-27632: Axxora #ALX-270-333-M025. Dissolve 25 mg with sterile water to a concentration of 5 mM; make 1 mL aliquots to store at -20°C. *Volumes to make 500 ml*: Complete DMEM 373 mL, F12 nutrient mix 125 mL, Hydrocortisone/EGF mix 0.5 mL, Insulin 0.5 mL, Fungizone/Amphotericin B 0.5 mL, Gentamicin 0.5 mL, Cholera toxin 4.3 uL, Y-27632 (add last) 0.5 mL.

Differentiation Media: bronchial epithelial growth medium (BEGM) supplemented with Ultroser G (BEGM/USG; Pall Corporation, Crescent Chemical Company). Contained 5 μg/ml insulin, 10 μg /ml transferrin, 0.07 μg /ml hydrocortisone, 0.6 μg/ml epinephrine, 0.8% vol/vol bovine hypothalamus extract, 0.5 mg/mL BSA, 0.5 μM ethanolamine, 15 ng/ml retinoic acid, 0.5 ng/ml human epidermal growth factor, 10 nM triiodothyronine, 0.5 μM phosphoethanolamine, and 0.5% vol/vol USG in Dulbecco's MEM (DMEM) + F12 nutrient mix.

Methods for measuring apical Tc-DTPA absorption in HNEs (cell ABS):

We measured the absorption rate of 99m Technetium labeled Diethylenetriamine pentaacetate (Tc-DTPA) from the apical surface of the HNEs (Cell ABS). This *in vitro* measurement parallels the measurement of Indium 111-DTPA absorption in the *in vivo* ABS measurement. Tc-DTPA was produced by adding 5 mCi Technetium 99m pertechnetate to a Draximage DTPA kit vial and adding saline until the total volume is 5ml. Strip chromatography was then performed to ensure proper binding. A volume of 10 μL of the Tc-DTPA solution was then diluted with 990 μL of Ringer's. A 10 μL volume of this diluted solution was added to the apical side of the HNEs (0.1 μCi of Tc-DTPA, DTPA mass=0.4 μg). Retained activity in the ASL, cell layer, and filter surface was measured by briefly withdrawing the filter and placing it above a rate counter and measuring emitted radioactive counts for 30 s. Measurements were made at=0, 2, 4, 6, 8, 12, and 24 hours. The normalized percentage of decay-corrected radioactive counts absorbed over 24 hours is reported as Cell ABS. Each reported measurement represents the average of 6 filters.

FRAP methods:

The ASL layer was labeled with 10 μL of 70 kDa FITC-labeled dextran (20 mg/mL, Sigma-Aldrich, St. Louis, MO). The following morning, 50 μL of perfluorocarbon (FC-770, ACROS organics, ThermoFisher, Waltham, MA) was applied to the apical surface to prevent evaporative losses during evaluation. The cultures were then placed on a modified stage of a Nikon TiE inverted microscope equipped with a Nikon confocal A1 scanner and the ASL was visualized with a 40× water immersion objective (Nikon Apo LWD 1.15 NA). A baseline image was obtained and then a small region (6 × 18 μm) in the middle of the ASL was photobleached for 400 milliseconds. Following photobleaching, serial images of the region were acquired. The data was fit to an exponential *rise to max* function to determine the time constant (τ) for fluorescence recovery associated with dye diffusion. FRAP is expressed as the ratio of the time constant of recovery in the ASL relative to saline (τ_{ASL}/τ_{saline}). Higher FRAP values are associated with longer diffusion times and slower diffusion rates.

Ussing Chamber measurements:

HNE monolayers cultured on filter supports (0.33-cm^2, Costar Transwell) were mounted in Ussing chambers and continuously short circuited with a VCC MC6 automatic voltage clamp (Physiologic Instruments, San Diego, CA) to measure their transepithelial short-circuit current (I_{sc}). Transepithelial resistance (TER), an indicator of monolayer integrity, was measured by applying a 2 mV bipolar pulse every 90 s at the start and end of the experiments and calculated using Ohm's law. A TER ≥ 200 Ωcm^2 was considered indicative of acceptable monolayer integrity. Ringer's solution composed of 115 mM NaCl, 25 mM $NaHCO_3$, 5 mM KCl, 10 mM HEPES, 1 mM $MgCl_2$, 1.5 mM $CaCl_2$, and 5 mM glucose was used to fill the apical and basolateral chambers, which were continuously gassed with a mixture of 95% O_2 and 5% CO_2 to maintain solution pH at 7.4. All experiments were performed at 37° C. Following chamber flooding and voltage clamping, the I_{sc} was allowed to

stabilize until a steady state was reached (~10-30 min). Next, amiloride (10 μM, apical) was added to block the flow of Na^+ through ENaC; the resulting change in Isc is reported as the Na^+ current. After 5 min, forskolin (10 μM, basolateral) was added to activate CFTR via its phosphorylation by protein kinase A; the Cl^- current is measured as the stimulated increase in Isc at its plateau, typically 3 min after addition of forskolin.

Sweat Chloride:

A Macroduct® system was used to collect sweat from the forearms of subjects after pilocarpine iontopheresis. The collection apparatus remained in place for 30 minutes. The procedure was performed on both arms. Samples were drawn from the Macroduct tubing for the measurement of Chloride concentration (mMol/L).

Multiple-breath washout (MBW):

MBW was performed with a photoacoustic spectroscopy system (Innocor, Innovision Medical, Denmark) and a re-breathing technique. The test gas mixture contained 0.2% sulfurhexafluoride (SF6) and air. After establishing a regular breathing pattern, the rebreathing bag was filled with the test gas. The subject breathed from this bag and wash-in is continued until an equilibrium was reached for a stable SF6 concentration. A valve then opened, and the patient breathed room air for the washout, which finished when the tracer gas (SF6) concentration fell below 2.5% (1/40) of the starting level. Functional residual capacity (FRC) was calculated from the cumulative volume of expired SF6 divided by the difference between end-tidal gas concentration at the start and end of the washout. Lung clearance index (LCI) was calculated as the cumulative expired volume, divided by the FRC. Three measurements were attempted and the average of 1-3 successful measurements was reported.

MCC/ABS nuclear scans:

Participants first lay recumbent while 4-minute anterior and posterior (256 x 256 pixel) background images were collected. A 90s Cobalt-57 transmission scan was then performed. These posterior images were used to locate the lung perimeter for use in subsequent analysis. Subjects then rose and were seated for radiopharmaceutical delivery. A DeVilbiss 646 nebulizer containing 1.5 mCi (55.5 MBq) of Indium 111-DTPA (In-DTPA) and 8 mCi (296 MBq) of Technetium 99m-sulfur colloid (Tc-SC) in 3 ml of normal saline was used. The nebulizer was driven by a DeVilbiss 8650D compressor attached through a Spira dosimeter which triggered the nebulizer for 0.7s after the participant had inhaled 100ml of air. Peak compressor flow during nebulization was 10-13 L/min. These methods were intended to preferentially deliver aerosol to the airways. Radiopharmaceutical delivery was performed for 2 minutes (ages 12 or 13) or 4 minutes (older participants). After delivery participants returned to the camera and lay recumbent for 80 minutes while a series of sequential images was collected. Imaging was conducted in three energy level windows: 140 keV (Tc99m), 210 keV (mid-window), and 247 keV (In111). Medium energy collimators were used. After 10 minutes of imaging, while continuing to lie in the camera, all participants inhaled nebulized isotonic saline using a special tubing arrangement. Aerosol was delivered for 10 minutes. Imaging continued throughout. On a separate study day (order randomized) the CF group inhaled 7% hypertonic saline (Pulmosal) during this period instead of isotonic saline.

Posterior right lung images were analyzed. The left lung was not used to avoid interference from the stomach. A whole lung region of interest (ROI) was drawn from the lung outline on the transmission scan and placed onto the clearance images and used to determine whole lung measurements (red outline on **Figure S2**). A rectangle was drawn that exactly surrounded this lung outline (blue dashed line box on Figure S2). Its size was then decreased to one-half of its original height and width. This box was placed at mid-height of the lung and designated as the central lung ROI (yellow box on Figure S2). The portion of the lung inside the whole lung region but outside of the central lung region was designated as the peripheral lung ROI. Central lung zones contain large and small airways and alveoli. Peripheral lung zones contain small airways and alveoli. No adjustment is made for peripheral lung clearance into the central lung zone.

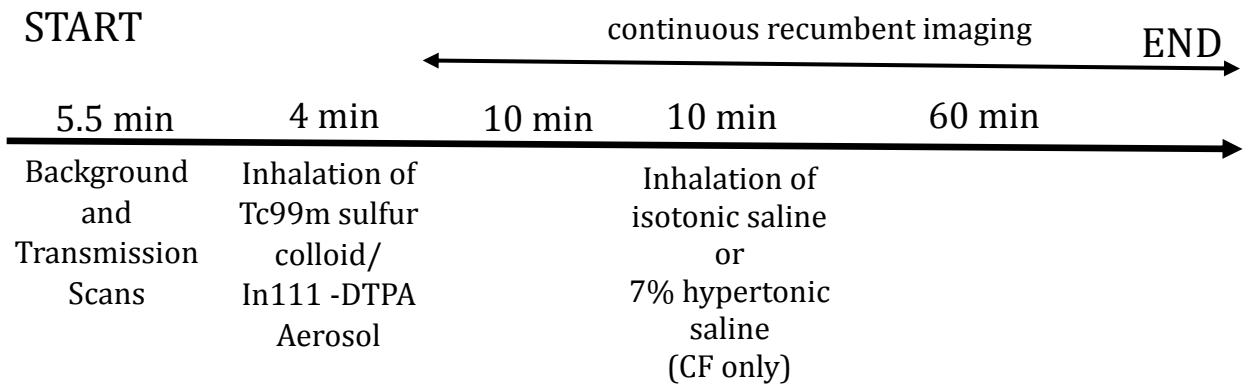

Figure S1: Timeline for imaging procedures. All subjects inhaled isotonic saline from a nebulizer while recumbent from t=10-20 min of the imaging period. CF subjects performed an additional imaging day where they inhaled 7% hypertonic saline during this period.

Measurements are adjusted for decay, background, and the spillover of Indium-111 into the Technetium-99m window. The latter correction was performed using the counts measured in the 210 KeV mid-window, which is midway between the two energy levels for In111 (173 and 247 KeV). Camera specific phantom studies were performed to determine the relative contributions of Indium 111 sources to the 140 KeV Tc99m window based on measures with known doses assessed in the 210 KeV window and the 140 KeV window.

Radioactive counts were normalized by starting counts in the ROI. MCC is the percentage of starting Tc-SC radioactive counts cleared at the end of the 80-minute study period, based on the average of the last 4 time points (t=74, 76, 78, and 80 min). Total In-DTPA clearance is the percentage of starting In-DTPA radioactive counts cleared at the end of the 80-minute study period, based on the average of the last 4 time points (t=74, 76, 78, and 80 min). ABS is total In-DTPA clearance minus MCC.

Adjusted MCC rate:

Previous studies have demonstrated that differences in the distribution of the deposited radioisotope aerosol in the lung can have a confounding effect on measurements of mucociliary

clearance (Locke et al, ERJ, 2016). Aerosol deposited in the larger, well-ciliated central airways is cleared more quickly that aerosol deposited in small airways or alveoli. To allow for comparisons of subjects with different distribution patterns we calculated an adjusted measure of MCC based on the amount of aerosol deposited in the central lung ROI (Cen%):

$MCC_{adjusted} = MCC_{measured} - S\ (Cen\% - Cen\%_{ave})$

where S is the slope of the relationship between $MCC_{measured}$ and Cen% in a multivariable model of MCC including central deposition % and group (HC, CR, or CF) as shown in table S2, S=1.33% cleared/% central deposition. Cen% is the subject's central deposition percentage and $Cen\%_{ave}$ is average of all three groups on the isotonic saline day (52%).

Use of $MCC_{adjusted}$ allows for comparisons between different subjects or different study days even if there is some variation in deposition pattern. It is utilized here to calculate MCC therapeutic response which involves two separate MCC measurements.

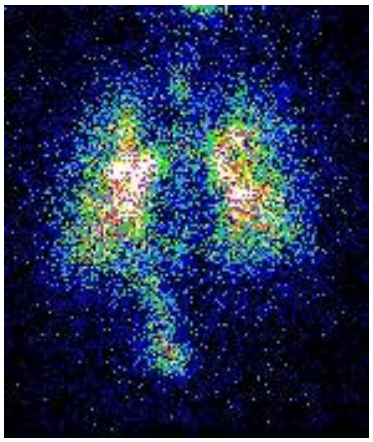

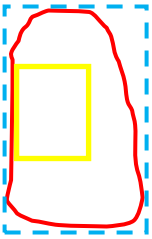

Figure S2: Regions of interest used for image analysis. Red is the whole lung region. Yellow is the central lung region. The peripheral lung region is the portion inside the whole lung but outside of central lung region. Technetium window shown.

Supplementary Data:

	Group I **CF ivacaftor (n=4)**	**Group TL** **CF ivacaftor + tezacaftor or lumacaftor (n=7)**	**Group N** **CF no corrector or potentiator (n=14)**	**All Groups** **p**	**I vs N** **p**	**TL vs N** **p**	**I vs TL** **p**
Age (years)	42 (27-61)	21 (17-39)	25 (18-31)	0.19	0.12	0.45	0.10
Female/male	1/3	2/5	9/5	0.45	0.26	0.36	0.29
FEV1 % pred	54 (48-83)	63 (47-73)	89 (67-98)	0.16	0.21	0.12	0.44
FVC % pred	86 (74-98)	89 (63-104)	102 (80-108)	0.51	0.43	0.46	0.48
FEF2575 % pred	25 (21-71)	26 (17-60)	59 (26-66)	0.39	0.39	0.30	0.43
LCI	13 (9-14)	9 (9-13)	9* (8-11)	0.31	0.25	0.30	0.31
Sweat Chloride (mMol/L)	25 (16-71)	95 (91-105)	107 (95-111)	0.06	**0.04**	0.13	0.22
MCC (WL)	46 (19-64)	27 (26-40)	40 (28-50)	0.39	0.41	0.32	0.26
MCC (PL)	46 (22-61)	27 (7-43)	37 (21-42)	0.33	0.25	0.27	0.24
MCC adjusted	34 (13-60)	26 (19-46)	38 (29-46)	0.63	0.37	0.50	0.68
ABS (WL)	5 (3-26)	24 (8-25)	23 (11-26)	0.56	0.43	0.47	0.37
ABS (PL)	9 (7-28)	27 (11-34)	18 (15-28)	0.54	0.44	0.29	0.40
% central aerosol deposition	55 (51-61)	51 (45-57)	51 (47-53)	0.44	0.36	0.44	0.24

Table S1: Comparing *in vivo* measurements in the CF group based on use of CFTR modulators. 4 CF subjects were using ivacaftor, 3 lumacaftor/ivacaftor, 4 tezacaftor/ivacaftor. 14 did not use modulators. 1 had unknown status. Data is Median (interquartile range). P values comparing all groups by Kruskal-Wallis (non-parametric). Group comparisons by Dunn's test with Holm correction (non-parametric, multiple comparisons). *-n=11.

Model Number	Model of	Central Deposition %		HC vs		Model		
		β	p	β	p	R^2	p	β 0
1	Whole Lung MCC	1.33	<0.001	CR -3.10 CF -7.02	0.55 0.19	0.23	0.01	-27
2	Peri Lung MCC	0.97	0.02	CR -3.02 CF -9.43	0.56 0.10	0.15	0.10	-10

Table S2: Multivariable linear regression model of mucociliary clearance (MCC) including central deposition percentage to indicate distribution of the aerosol and comparing healthy controls (HC), to Cystic Fibrosis (CF) and carrier (CR) groups.

	CF (n=26) IS	CR (n=16)	HC (n=12)	CF (n=26) HS	p	p(CFvHC)	p(CFvCR)	p(CRvHC)	p CF (HSvIS)
MCC (WL) ADJ	36 (23-46)	35 (30-48)	39 (34-52)	51 (40-62)	0.38	0.26	0.49	0.25	0.0002

Table S3: Adjusted mucociliary clearance (MCC) measurement. Since deposition of the radioisotope aerosol can affect measurements of MCC we calculated an adjusted MCC based on the slope of the relationship between MCC and central deposition %.

The formula used was MCC adjusted = $MCC_{measured} - S (Cen\% - Cen\%_{ave})$ where S is the slope of the relationship between MCC measured and Cen% in the multivariable model shown in Table S2, S=1.33% cleared/% central deposition. Cen% is the subject's central deposition percentage and $Cen\%_{ave}$ is average of all three groups on the isotonic saline day (52%).

All groups inhaled isotonic saline (IS) during the MCC/ABS scan. CF subjects performed an additional study day where they inhaled 7% hypertonic saline (HS) during the scan.

Data is Median (interquartile range). P values comparing all groups by Kruskal-Wallis (non-parametric). Group comparisons by Dunn's test with Holm adjustment (non-parametric, multiple comparisons). HS vs IS comparison for CF group by Wilcoxon matched-pairs signed-ranks test (non-parametric, paired).

CF=cystic fibrosis, CR=single CFTR disease-causing mutation (parents of CF participants), HC=healthy controls, HS=hypertonic saline (7%), IS=isotonic saline (0.9%). WL=whole lung, PL=peripheral lung, ADJ= adjusted values based on % of central lung aerosol distribution. Cen %=percentage of whole lung radioactive counts found in the central lung zone.

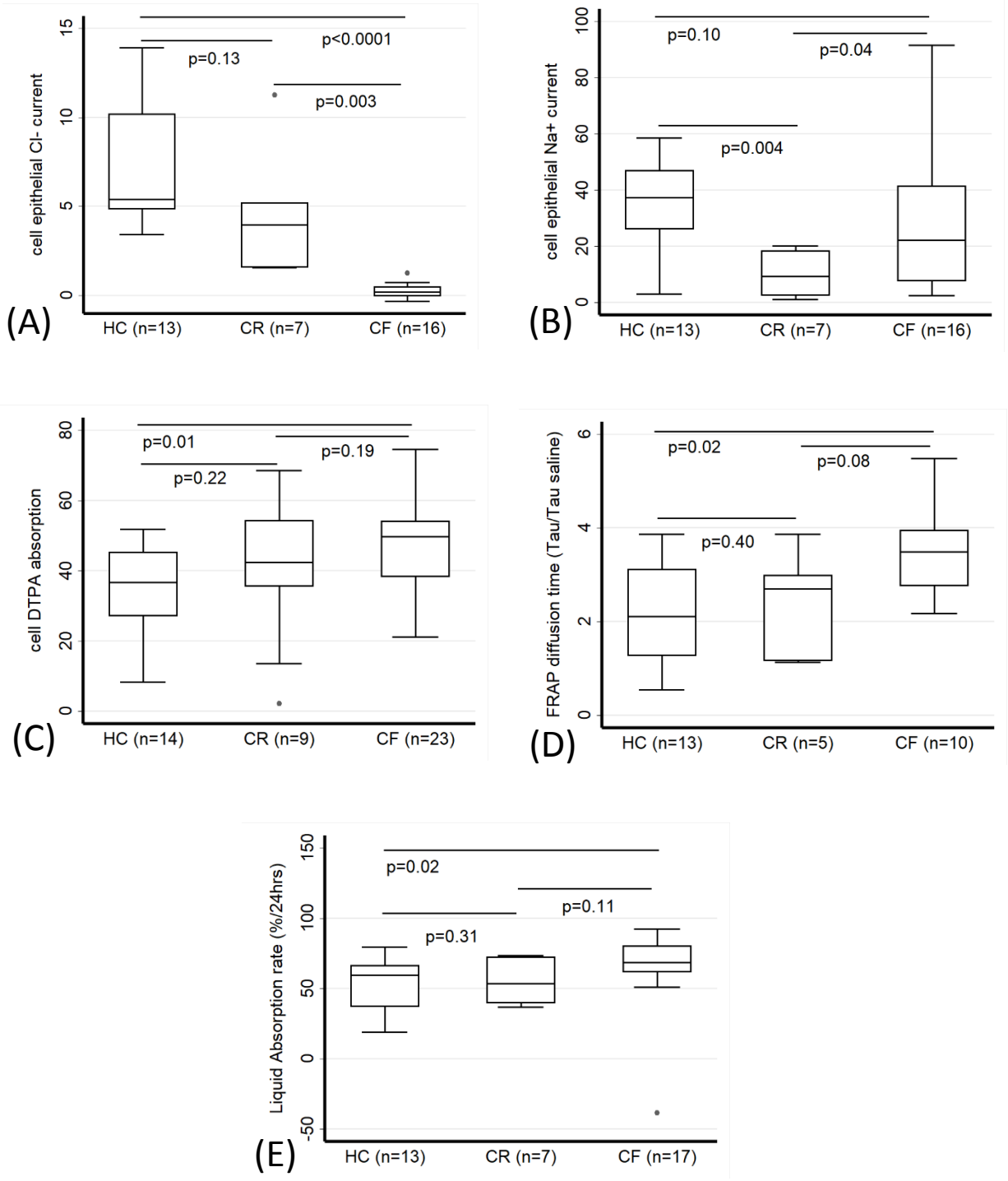

Figure S3: Graphical comparisons of *in vitro* measurements from HNE cultures presented in table 2. (A) Epithelial Cl- current from Ussing chamber. (B) Na+ current, (C) Cell ABS = Tc-DTPA absorption rate from apical surface of cells (% cleared/24 hrs.) (D) Fluorescence recovery after photobleaching (FRAP). (E) Airway surface liquid absorption rate (%/24hrs) as measured using an optical method Ref. 6) Group comparisons by Dunn's test with Holm adjustment (non-parametric, multiple comparisons).

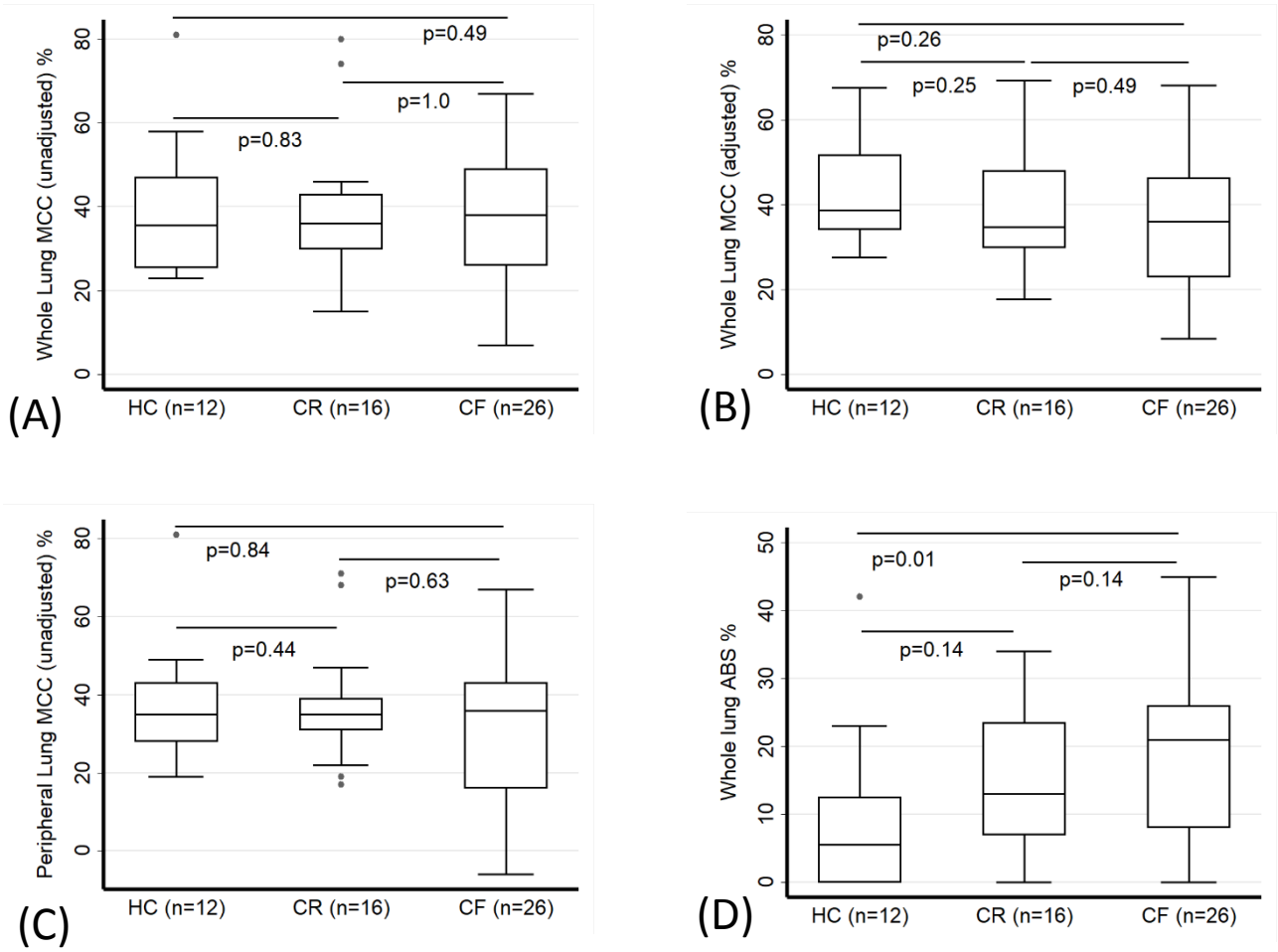

Figure S4: Graphical comparisons of *in vivo* imaging measurements presented in table 3. (A) Mucociliary clearance rate (MCC) for the whole lung region, (B) MCC for the whole lung region adjusted for aerosol distribution, (C) MCC for the peripheral lung region (unadjusted), (D) ABS – absorptive component of Indium 111-DTPA clearance. Group comparisons by Dunn's test with Holm adjustment (non-parametric, multiple comparisons).

(A)

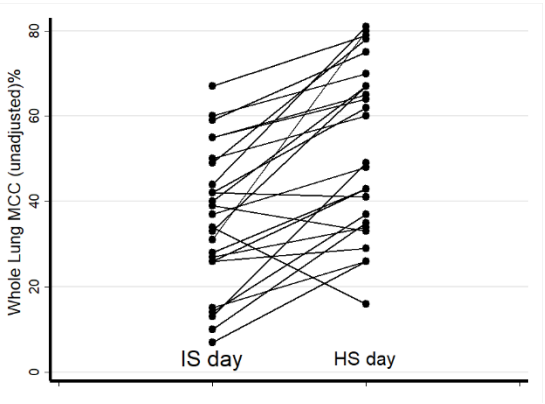

(B)

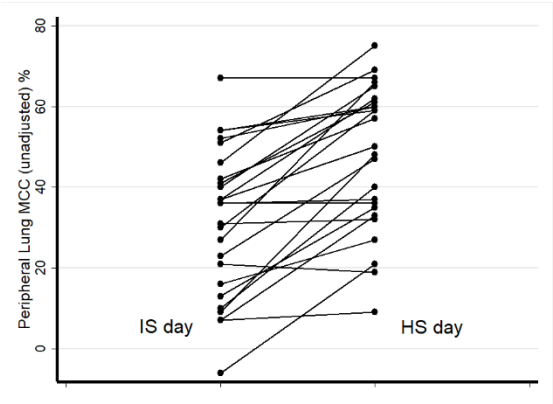

(C)

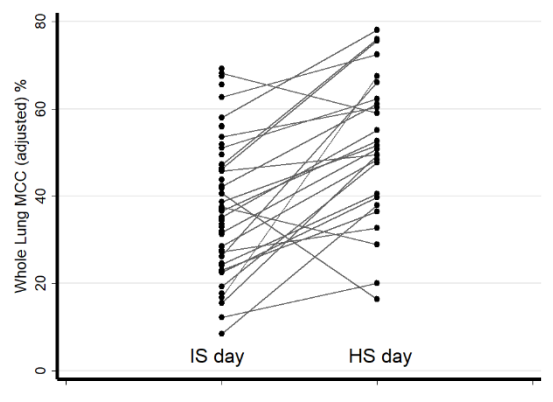

Figure S5: Mucociliary clearance (MCC) in CF group comparing inhalation of isotonic saline (IS day) to hypertonic saline (HS day). (a) Whole lung MCC with no adjustment for aerosol distribution ($p=0.0001$), (b) peripheral lung MCC with no adjustment ($p<0.0001$), (c) whole lung clearance adjusted for aerosol distribution ($p=0.0002$). Comparisons by Wilcoxon matched-pairs signed-ranks test (non-parametric, paired).

Study number UNIT	CF control carrier	CFTR allele 1	CFTR allele 2	Age	Gender	cell DTPA absorption (%/24 hrs)	TER (Ohm cm^2)	cell epithelial Na+ current (uA/cm^2)
UHC 1	control	WT	WT	23	M	27.1	522	54
UHC 2	control	WT	WT	20	M	38.2	753	43
UHC 3	control	WT	WT	20	M	35.3	495	45
UHC 4	control	WT	WT	20	M	15.8	248	3
UHC 5	control	WT	WT	22	M	39.7	556	37
UHC 6	control	WT	WT	23	M	20.8	787	8
UHC 7	control	WT	WT	23	M	28.1	655	26
UHC 9	control	WT	WT	20	M	45.2	515	34
UHC 10	control	WT	WT	25	F	28.6	499	47
UHC 11	control	WT	WT	22	F	51.8	589	32
UHC 12	control	WT	WT	23	F	50.1	673	51
UHC 13	control	WT	WT	29	F	8.3	687	59
UHC 14	control	WT	WT	27	F	47.4		
UHC 16	control	WT	WT	19	F	43.4	294	21
UP 1	carrier	WT	F508del	47	F			
UP 2	carrier	WT	p Pro574His	36	F			
UP 3	carrier	WT	F508del	35	M	68.5	384	9
UP 4	carrier	WT	del exon 22 23	41	F			
UP 5	carrier	WT	S549N	48	F	2.2	717	1
UP 6	carrier	WT	F508del	47	M	61.6	109	12
UP 7	carrier	WT	F508del	48	M	46.1	1334	20
UP 8	carrier	WT	F508del	72	F			
UP 9	carrier	WT	F508del	73	M	13.6	205	2
UP 10	carrier	WT	F508del	64	F			
UP 11	carrier	WT	F508del	53	F	36.1	762	18
UP 12	carrier	WT	2184insA	56	F	35.6	1066	5
UP 13	carrier	WT	F508del	70	M			
UP 14	carrier	WT	R334W	63	F			
UP 15	carrier	WT	R553X	44	F	54.3		
UP 16	carrier	WT	F508del	44	M	42.4		
UCF 1	CF	F508del	F508del	21	M	39.5	1229	26
UCF 2	CF	F508del	p Pro574His	15	M			
UCF 3	CF	F508del	N1303K	13	M	56.6	325	6
UCF 4	CF	c.1585-2A>G	p.G551D	25	F			
UCF 5	CF	F508del	del exon 22 23	26	F	46.8		

UCF 6	CF	F508del	S549N	29	M	38.2	1170	58
UCF 8	CF	F508del	del e2, e3	31	M	56.1	610	54
UCF 9	CF	F508del	N1303K	24	F	54.1	692	43
UCF 10	CF	F508del	D1152H	67	M	56.2	492	25
UCF 11	CF	F508del	F508del	14	F	55.1	414	5
UCF 12	CF	F508del	W1282X	39	F	74.5	194	3
UCF 13	CF	F508del	F508del	31	F	53.8	322	33
UCF 14	CF	F508del	F508del	40	M	36.5	520	8
UCF 15	CF	F508del	F508del	17	M	51.3	752	19
UCF 16	CF	F508del	F508del	21	M	49.7	774	91
UCF 17	CF	F508del	F508del	49	F	32.7	1746	19
UCF 18	CF	F508del	F508del	39	F	51.6	792	8
UCF 19	CF	F508del	D579G	29	F	52.0		
UCF 20	CF	F508del	2184insA	18	F	54.0	821	40
UCF 21	CF	F508del	R117H	55	M	44.7	528	13
UCF 22	CF	F508del	R334W	41	M	41.4		
UCF 23	CF	F508del	F508del	27	F	33.7		
UCF 24	CF	F508del	R553X	12	F	45.2		
UCF 25	CF	F508del	E60X	19	F	21.2		
UCF 26	CF	F508del	F508del	39	F	34.1		
UCF 27	CF	F508del	2183delAA-G	23	M			

cell epithelial Cl- current (uA/cm^2)	cell FRAP (Tau/Tau saline)	PFT - FEV1per day1 %p	PFT - FVCper day1 %p	PFT - FEF25_75per day1 %p	whole lung TC clear isot %/100
8	1.6	104	107	94	0.38
5	3.0	100	108	73	0.25
5	2.1	89	93	77	0.33
11	0.5	115	120	103	0.24
5	3.5	77	79	68	0.27
13	0.6	110	104	120	0.26
5	1.2				
4	3.1	95	116	62	0.39
5	1.3	114	100	68	0.58
8	3.4	96	116	61	0.81
10	2.2	112	113	119	0.44
14	2.1	114	125	89	0.23
3	3.9	96	100	96	0.50
		106	112	91	0.74
		121	121	125	0.31
4	3.0	71	105	31	0.80
		125	120	141	0.43
2	1.1	94	96	104	0.34
11	2.7	113	116	255	0.21
5	3.9	92	104	65	0.43
		112	104	164	0.27
4	1.2	94	95	94	0.32
		85	91	59	0.46
2		99	99	111	0.33
4		104	106	101	0.15
		98	95	114	0.38
		94	96	100	0.38
		96	100	83	0.43
		90	104	58	0.29
0		63	104	60	0.40
		127	133	117	0.28
0	3.1	116	108	149	0.42
		108	105	114	0.60
		67	76	46	0.55

1		50	80	22	0.07
0	2.3	87	101	54	0.39
0	3.6	76	80	64	0.55
0	4.9	58	91	28	0.31
0	3.4	73	127	23	0.49
0	2.2	36	48	12	0.40
1	3.6	40	62	12	0.50
0	2.8	53	67	26	0.26
0	4.0	93	98	83	0.27
1	5.5	68	89	35	0.10
0		48	79	15	0.44
0		31	40	15	0.26
		92	103	63	0.34
0		98	103	94	0.14
1		45	67	19	0.67
		64	92	23	0.59
		47	63	17	0.33
		98	111	66	0.42
		71	97	26	0.13
		90	104	48	0.37
		95	109	66	0.15

whole lung IN clear isot %/100	central lung Tc clear isot %/100	central lung In clear isot %/100	peripheral lung Tc clear isot %/100	peripheral lung In clear isot %/100	central % Tc isot %
0.43	0.34	0.42	0.42	0.43	49
0.48	0.13	0.36	0.34	0.57	45
0.45	0.29	0.33	0.36	0.53	46
0.34	0.20	0.30	0.27	0.36	44
0.32	0.25	0.32	0.29	0.33	49
0.68	0.35	0.69	0.19	0.67	46
0.40	0.45	0.37	0.33	0.43	54
0.49	0.71	0.51	0.43	0.47	54
0.58	0.80	0.51	0.81	0.65	62
0.40	0.46	0.37	0.43	0.43	49
0.35	0.25	0.30	0.20	0.39	49
0.47	0.51	0.49	0.49	0.46	47
0.65	0.76	0.67	0.71	0.62	58
0.55	0.27	0.42	0.35	0.65	44
0.80	0.87	0.85	0.68	0.73	60
0.56	0.47	0.54	0.39	0.59	49
0.57	0.32	0.60	0.35	0.55	39
0.42	0.24	0.41	0.19	0.43	41
0.56	0.47	0.55	0.39	0.56	51
0.53	0.23	0.54	0.33	0.50	54
0.66	0.30	0.70	0.35	0.62	55
0.52	0.45	0.54	0.47	0.47	61
0.42	0.37	0.47	0.29	0.34	53
0.45	0.13	0.45	0.17	0.45	50
0.51	0.50	0.59	0.22	0.39	56
0.46	0.40	0.48	0.34	0.40	62
0.53	0.46	0.54	0.39	0.53	47
0.25	0.23	0.23	0.36	0.27	50
0.46	0.38	0.56	0.43	0.35	47
0.54	0.43	0.51	0.13	0.56	52
0.73	0.53	0.79	0.31	0.65	49
0.62	0.64	0.62	0.54	0.62	59
0.70	0.58	0.73	0.52	0.68	46

0.52	0.07	0.51	0.07	0.52	51
0.62	0.41	0.69	0.36	0.53	53
0.56	0.56	0.60	0.54	0.50	53
0.34	0.28	0.26	0.37	0.47	63
0.57	0.53	0.57	0.46	0.57	45
0.51	0.40	0.49	0.40	0.55	55
0.62	0.55	0.71	0.42	0.48	63
0.50	0.37	0.52	0.09	0.47	62
0.44	0.55	0.57	-0.06	0.28	54
0.39	0.14	0.39	0.07	0.39	45
0.61	0.53	0.66	0.30	0.51	61
0.51	0.16	0.43	0.36	0.59	51
0.58	0.48	0.67	0.21	0.48	47
0.43	0.19	0.44	0.10	0.42	46
0.74	0.66	0.75	0.67	0.73	51
0.61	0.65	0.60	0.51	0.63	61
0.57	0.38	0.59	0.27	0.55	57
0.61	0.44	0.62	0.41	0.59	52
0.38	0.02	0.38	0.23	0.39	50
0.61	0.38	0.62	0.37	0.59	51
0.45	0.13	0.47	0.16	0.44	46

central % In iso	whole lung ABS Isot	central lung ABS Isot	peripheral lung ABS Isot	whole lung Tc clear HS	whole lung In clear HS
%	%/100	%/100	%/100	%/100	%/100
48	0.05	0.09	0.01		
42	0.23	0.22	0.22		
38	0.13	0.04	0.17		
45	0.10	0.10	0.09		
52	0.06	0.08	0.04		
48	0.42	0.34	0.48		
55	0.01	0.00	0.10		
54	0.00	0.00	0.04		
51	0.00	0.00	0.00		
44	0.00	0.00	0.00		
50	0.12	0.05	0.18		
51	0.00	0.00	0.00		
62	0.00	0.00	0.00		
44	0.24	0.16	0.30		
62	0.01	0.00	0.04		
54	0.13	0.07	0.20		
34	0.23	0.28	0.20		
45	0.21	0.17	0.24		
56	0.13	0.08	0.18		
59	0.25	0.32	0.17		
58	0.34	0.40	0.27		
63	0.06	0.09	0.00		
58	0.08	0.10	0.05		
54	0.30	0.32	0.28		
60	0.13	0.08	0.17		
69	0.08	0.07	0.06		
48	0.11	0.08	0.14		
52	0.00	0.00	0.00		
54	0.06	0.18	0.00	0.77	0.81
47	0.26	0.09	0.43	0.43	0.57
61	0.31	0.26	0.34	0.41	0.60
65	0.02	0.00	0.08	0.70	0.74
50	0.15	0.15	0.16	0.65	0.75

50	0.45	0.45	0.45	0.26	0.60
56	0.23	0.27	0.17	0.33	0.62
55	0.00	0.04	0.00	0.64	0.73
61	0.03	0.00	0.10	0.80	0.76
51	0.08	0.04	0.11	0.78	0.86
57	0.11	0.09	0.15	0.67	0.71
61	0.11	0.15	0.06	0.60	0.64
62	0.24	0.15	0.38	0.43	0.73
56	0.17	0.02	0.34	0.34	0.57
48	0.29	0.26	0.32	0.35	0.66
64	0.17	0.13	0.22	0.81	0.87
47	0.25	0.27	0.23	0.29	0.53
50	0.24	0.19	0.27	0.16	0.48
48	0.29	0.25	0.32	0.37	0.56
59	0.07	0.09	0.05	0.79	0.75
63	0.02	0.00	0.12	0.75	0.84
63	0.24	0.21	0.27	0.67	0.84
61	0.19	0.19	0.19	0.62	0.84
54	0.26	0.36	0.16	0.49	0.73
55	0.23	0.24	0.22	0.48	0.73
47	0.31	0.34	0.28	0.26	0.64

central lung Tc clear HS %/100	central lung In clear HS %/100	peripheral lung Tc clear HS %/100	peripheral lung In clear HS %/100	Central % Tc HS %	Central % In HS %
0.75	0.85	0.79	0.77	53	56
0.52	0.64	0.35	0.49	48	49
0.52	0.63	0.32	0.57	46	51
0.78	0.78	0.59	0.70	58	58
0.70	0.81	0.60	0.70	46	49

0.48	0.74	0.09	0.50	43	45
0.29	0.61	0.37	0.63	55	57
0.67	0.76	0.60	0.69	55	55
0.91	0.82	0.62	0.65	61	61
0.81	0.91	0.75	0.75	52	69
0.69	0.80	0.65	0.47	63	71
0.62	0.67	0.57	0.60	56	54
0.41	0.78	0.48	0.61	69	69
0.48	0.66	0.21	0.47	47	50
0.38	0.63	0.33	0.68	42	44
0.88	0.91	0.59	0.70	75	77
0.21	0.47	0.36	0.60	49	51
0.14	0.47	0.19	0.49	52	52
0.34	0.60	0.40	0.51	50	55
0.85	0.81	0.67	0.68	67	57
0.80	0.89	0.69	0.77	51	61
0.67	0.86	0.66	0.82	53	55
0.62	0.86	0.61	0.82	53	55
0.50	0.77	0.47	0.68	52	58
0.46	0.75	0.50	0.71	49	55
0.25	0.63	0.27	0.65	44	45

Whole lung ABS HS %/100	Central lung ABS HS %/100	Peripheral lung ABS HS %/100	Corrector potentiator name	RACE	hispanic=1
				C	0
				C	0
				C	0
				C	0
				ASA	0
				C	0
				C	0
				C	0
				AA	0
				ASA	0
				C	0
				C	0
				C	0
				C	0
				C	0
				C	0
				C	0
				C	0
				C	0
				C	1
				C	0
				C	0
				C	0
				C	0
				C	0
				C	0
				C	0
				C	0
				C	1
				C	1
				C	0
0.04	0.10	-0.02	Luma/Iva	C	0
0.13	0.12	0.15	No	C	0
0.19	0.12	0.25	No	C	0
0.04	-0.01	0.11	Iva	C	0
0.11	0.11	0.10	No	C	0

0.35	0.26	0.41	Iva	C	1
0.29	0.32	0.26	No	C	0
0.09	0.09	0.09	No	C	0
-0.04	-0.08	0.03	Iva	C	0
0.08	0.10	0.00	Luma/Iva	C	0
0.03	0.11	-0.18	No	C	0
0.04	0.05	0.03	No	C	0
0.30	0.37	0.13	Teza/Iva	C	0
0.23	0.18	0.26	Teza/Iva	C	0
0.31	0.25	0.34	Luma/Iva	C	0
0.06	0.03	0.11		C	0
0.25	0.26	0.24	Teza/Iva	C	0
0.31	0.33	0.30	No	C	0
0.18	0.25	0.11	No	C	0
-0.04	-0.04	0.01	Iva	C	0
0.09	0.08	0.08	No	C	1
0.17	0.19	0.16	Teza/Iva	C	0
0.22	0.23	0.21	No	C	0
0.24	0.27	0.20	No	C	0
0.25	0.29	0.21	No	C	0
0.38	0.38	0.39	No	C	0

sweat chloride mMol/L	acute PA infection==1	acute mrsa=1	acuite staph=1	chronic PA =1	chronic MRSA =1	chronic staph =1
26						
39						
24						
20						
10						
46						
14						
10						
32						
10						
10						
24						
26						
21						
48						
14						
53						
58						
55						
21						
52						
40						
53						
17						
31						
13						
92	1	1	0	1	1	0
59	0	0	1	0	0	1
104	0	0	1	0	0	1
14	0	0	0	0	0	0
108	0	1	0	0	1	0

110	1	0	1	1	0	1
111	1	0	0	1	0	0
110	0	0	1	0	0	1
32	0	0	0	0	0	0
89	0	0	0	0	0	0
120	0	0	1	1	1	0
94	1	0	0	1	1	0
105	1	0	0	1	0	0
101	0	1	0	0	1	0
119	0	0	1	0	0	1
99						
91	0	0	0	1	0	0
70				1	0	0
105	1	0	0	0	0	1
18	1	0	0	1	0	0
95	1	0	1	1	0	1
95	1	1	0	1	1	0
121	0	0	0	0	0	1
115				0	1	0
111	0	0	0	0	0	1
101	0	0	0	0	0	0

ave FRC from MBW testing	average lci from mbw testing	PAPER liq abs rate 0 %/100 over 24rs	heightcm	weightkg	PAPER MCC adjusted %
3.5	6.7	0.23	187	83	42
2.6	6.7	0.67	180	87	35
2.5	7.3	0.38	182	94	40
3.2	9.4	0.68	185	85	35
2.8	7.5	0.60	177	79	31
4.8	6.3	0.37	184	80	34
		0.62			
3.1	7.2	0.59	176	71	37
1.9	8.1	0.19	163	68	56
3.2	7.3	0.79	159	47	68
2.5	7.1	0.68	159	57	47
		0.27	173	84	28
2.2	6.2	0.41	166	75	56
2.6	6.7		163	112	66
2.8	7.3		169	84	42
3.2	8.0	0.40	178	77	69
2.8	8.3		168	76	46
2.1	6.9	0.37	149	77	52
2.9	6.7	0.65	173	83	35
3.7	7.9	0.72	185	93	44
1.8	7.5		155	74	25
2.4	8.9	0.54	165	85	28
2.0	8.3		160	91	34
2.7	7.9	0.73	159	61	31
2.3	7.9	0.53	165	79	18
4.4	6.9		169	73	33
1.7	9.0		157	60	24
2.0	7.4		162	71	50
3.5	8.3		168	62	32
2.2	8.9	0.69	178	72	46
3.1	6.5		178	97	29
2.0	7.3	0.51	151	38	46
2.3	6.5		162	63	51
1.4	8.6		171	56	63

1.3	14.3	0.67	192	67	9
2.3	9.8	0.61	172	86	38
		0.73	154	57	54
3.5	13.6	0.80	172	61	17
2.1	9.0	0.66	151	61	58
1.5	8.7	0.76	152	85	37
1.6	12.6	0.85	144	44	35
2.1	13.0	0.63	186	92	12
2.8	6.7	0.62	179	72	24
3.5	9.0	0.91	171	63	19
2.1	15.0	0.61	156	53	32
1.0	15.7	0.92	163	44	27
1.8	7.6	0.84	157	85	41
1.9	7.5	0.68	161	61	22
1.7	12.4	-0.38	167	95	68
3.1	8.9		173	73	47
1.2	11.2		159	49	26
			147	36	42
			151	43	15
1.5	13.1		165	69	39
3.2	11.2		177	78	23

PAPER HS MCC adjusted %	PAPER therapeutic respons %
76	29
48	20
50	4
62	11
72	10

38	29
29	-9
60	7
68	51
78	20
53	16
55	20
20	8
41	16
48	28
51	19
33	5
16	-24
40	17
59	-9
76	29
66	40
61	19
49	34
52	13
36	13